

# Depth Filtration: Fundamental Investigation through Three-Dimensional Trajectory Analysis

ROBERT S. CUSHING\*

Carollo Engineers, 12426 West Explorer Drive, Suite 200, Boise, Idaho 83713

DESMOND F. LAWLER

University of Texas, Department of Civil Engineering, Austin, Texas 78712

A mathematical model (array of spheres or AOS Model) of aqueous depth filtration was developed using trajectory analysis performed on a porous media model comprised of a face-centered cubic packing of spheres. To extend removal efficiency predictions beyond the grain-size scale and take into account the presence of densely and sparsely packed regions in an actual filter bed, a parallel deficit porosity compensation scheme was developed and applied. A correlation for single collector efficiency was developed from trajectory results and, using the parallel deficit porosity compensation scheme, compared to an existing model and experimental results. Although the model discussed herein was developed with the intent of advancing the understanding of depth filtration, this work offers tools for investigating and insights into particle fate and transport in other circumstances, e.g., groundwater aquifers. This model represents the first use of a porous media model that explicitly accounts for grain contact points for trajectory modeling of aqueous depth filtration. Particle collection within the model was strongly associated with grain contact points, a phenomenon due largely to hydrodynamic forces "funneling" particles to trajectories coincident with grain contact points. In comparison to previous trajectory models, this model is less sensitive to particle size and filtration rate and much less sensitive to surface chemistry than other currently available models. At moderate to high filtration rates (on the order of 3.7 mm/s or 5.4 gpm/ft<sup>2</sup>), the AOS model represented well experimental data for removal of particles less than 5 μm. At lower filtration rates and larger particle sizes, the AOS model tends to overpredict particle removal.

## Introduction

Depth filtration is the solid/liquid separation process in which a suspension, generally dilute, is passed through a packed bed of sand, anthracite, or other granular media. Solids (particles) attach to the media or previously retained particles and are removed from the fluid. Because of public health concerns and regulatory pressure, filtration is virtually ubiquitous in the treatment of surface waters for potable

water supply. Depth filtration is also often successfully used as a tertiary treatment for wastewater. The process has been used for centuries and has been studied quite extensively; however, on a fundamental level, depth filtration is very complex, and understanding is still limited. Since filtration is often the final particle removal process, unit process failure results in overall plant failure; conversely, if the filtration process is operating properly, effects of unit process failure upstream can be mitigated by filtration.

Performance of a filter is quantified by particle removal and head loss across the packed bed. In water and wastewater treatment, particle removal or effluent quality must meet or exceed a specified standard throughout the dynamic cycle of ripening (often observed initial increase in removal efficiency) and breakthrough (deteriorating effluent quality). The duration of a filter run is limited by numerous constraints: available head, effluent quality, or flow requirement. The head loss and removal efficiency of a filter are complicated functions of suspension qualities (particle size distribution and concentration, particle surface chemistry, and solution chemistry), filter design parameters (media size, type, and depth), and operating conditions (filtration rate and filter runtime). Adequate predictive models are not yet available for use within a rational design framework, and hence, conservative designs or extensive pilot studies are required to develop design parameters. Responses to changes in influent quality or operating parameters are currently impossible to predict.

The grains and pores of a deep bed filter form a complex, random structure, and the hydrodynamics of the system cannot be described exactly in a mathematical framework at this time. The complexity of the system leads to two possible approaches to the problem: the physical system can be approximated crudely enough that an exact mathematical solution to the problem is feasible, or a more accurate representation of the system can be used that requires an approximate mathematical solution. Previous research has been performed using media models following the former approach, while the research discussed herein follows more closely the latter. Specifically, trajectory analysis was performed using a media model that explicitly accounts for grain contact points; the packed bed was modeled as a face-centered cubic array of spheres. However, unlike previously implemented media models that possess geometries simple enough to be solved exactly under Stokes' flow assumptions, the solution applied to the flow field within the array of spheres media model is an approximation.

Although representation of grain packing as a uniform lattice of spheres is much simpler than the random packing of nonuniform grains in an actual filter bed, it shares with an actual filter the important feature of contact points among grains. Effects of filter grain contact points on particle collection have not been considered explicitly in previous models of deep bed filtration. The specific objectives of this research were to develop a mathematical model of initial removal in a deep bed filter based on trajectory analysis performed on a media model comprised of dense periodic packing of spheres and couple the trajectory results with an appropriate representation of the entire filter bed. Description and results of the resulting model of aqueous depth filtration, referred to as the array of spheres (AOS) model, are presented below.

## Modeling Approach

**Background.** Depth filtration has been investigated extensively through mathematical modeling. The first math-

\* Corresponding author phone: (208)376-2288; fax: (208)376-2251; e-mail: rcushing@carollo.com.

emtical description of depth filtration was formulated by Iwasaki (1). Through extensive experimental observation and deductive reasoning, Iwasaki developed relationships describing the operation of deep bed filters. Originally expressed as a set of partial differential equations and cast in terms of particle flux, Iwasaki's equations are generally written in modern filtration literature in terms of number concentration rather than flux. Under clean bed conditions, the set of partial differential equations condense to a single first-order ordinary differential equation:

$$\frac{dN}{dz} = -\lambda_0 N \quad (1)$$

where  $z$  is the media depth (L),  $\lambda_0$  is the initial filter coefficient ( $L^{-1}$ ), and  $N$  is the particle number concentration (number  $L^{-3}$ ).

Currently, the only predictive approach to modeling removal of non-Brownian particles in depth filtration is trajectory analysis. In trajectory analysis, a simplified model of the filter bed and associated flow field is selected, and through resolution of forces and torques on a particle in the system, the trajectory of that particle can be determined. The particle trajectory determines the fate of the particle, i.e., retention on the filter media or passage through the system. Trajectory analysis is an approach that has led to considerable insight toward depth filtration and is a method of predicting a priori the initial (clean bed) filter coefficient ( $\lambda_0$  in eq 1).

Yao et al. (2) presented the first use of trajectory analysis in modeling deep bed filtration of hydrosols, applying an isolated sphere under Stokes' flow to represent the hydrodynamics of the flow near a single filter grain. Subsequently, researchers have performed trajectory analysis using porous media models that account for neighboring grains, most notably, sphere-in-cell (3–7) and constricted tube (8, 9). Note that these models were originally developed as a means of estimating head loss across packed beds, and later, filtration researchers adopted these models for use in conjunction with trajectory analysis calculations.

Rajagopalan and Tien (4, 5) correlated trajectory analysis results with dimensionless groups for gravity ( $N_G$ ), particle–collector ratio ( $N_R$ ), and London attraction ( $N_{Lo}$ ) to obtain the unit collector efficiency due to sedimentation and interception. The correlation in terms of single collector efficiency ( $\eta_{s(S\&I)}$ ) may be expressed as

$$\eta_{s(S\&I)} = A_s N_{Lo}^{0.125} N_R^{1.875} + 0.003375 A_s N_G^{1.2} N_R^{-0.4} \quad (2)$$

where  $A_s$  is the Happel's flow parameter:

$$A_s = \frac{2(1-p^5)}{w} \quad (3)$$

and  $p = (1 - \epsilon)^{1/3}$ ,  $w = 2 - 3p + 3p^5 - 2p^6$ , and  $\epsilon$  is the porosity.

$$N_{Lo} \text{ (London group)} = \frac{4H}{9\pi\mu d_p^2 V_o} \quad (4)$$

$$N_R \text{ (relative size group)} = \frac{d_p}{d_c} \quad (5)$$

$$N_G \text{ (gravity group)} = \frac{d_p^2(\rho_p - \rho_f)g}{18\mu V_o} \quad (6)$$

where  $H$  is the Hamaker's constant;  $d_p$  is the particle diameter;  $d_c$  is filter media grain (collector) diameter;  $\rho_p$  and  $\rho_f$  are particle and fluid viscosity, respectively;  $g$  is the gravitational constant;

$\mu$  is the fluid viscosity; and  $V_o$  is the superficial velocity. As the correlation of trajectory analysis results presented in eq 2 includes only deterministic (or nondiffusional) collection terms, collection due to diffusion was included by adding the following term for single collector efficiency due to diffusion (10):

$$\eta_d = 4Pe^{-2/3} A_s^{1/3} \quad (7)$$

where  $\eta_d$  is the diffusional collection (collection by Brownian motion),  $Pe$  is the Peclet number  $[(d_c V_o)/D_{BM}]$  with  $D_{BM}$  as the particle diffusion coefficient  $[kT/(3\pi\mu d_p)]$ ,  $k$  as the Boltzmann's constant, and  $T$  as the absolute temperature.

A primary drawback of current media models when applied to trajectory analysis is the failure to explicitly account for grain contact points. Porous media models that have been implemented for trajectory analysis of hydrosols are similar in that specific grain interactions, i.e., flow field and geometric features induced by grain contact points and proximity, are not explicitly taken into account. In existing models, the filter grains (isolated sphere and sphere-in-cell models) or pores (capillary and constricted tube models) are represented by geometries that are solids (or voids) of revolution. Thus, the velocity profiles are also surfaces of revolution, and two-dimensional trajectory analysis is sufficient to define all particle trajectories.

One method of taking into account collector–collector interactions is to model the filter media as an array of regularly packed spheres. Although a regular packing arrangement of spheres does not represent exactly the random packing and often nonuniform grains of an actual filter, it allows a more realistic representation of the geometry and flow field than current media models. Gal et al. (12) used a face-centered cubic packing of spheres to represent the media in examining aerosol filtration. The flow field was determined using a modified form of the solution method of Snyder and Stewart (13). The results predict higher collection efficiencies than other models and correlate much better with experimental results.

In aerosol filtration, particle inertia is significant, and inertial impaction is generally the dominant collection mechanism; however, in depth filtration of particles from water, particle inertia is negligible, and inertial impaction is not a significant collection mechanism. Since their research concerned aerosol filtration, Gal et al. (12) included deposition by inertial impaction and neglected gravitational effects. Also, Gal et al. (12) did not consider hydrodynamic interactions, an important element for refining the precision of trajectory calculations performed on hydrosols. Hence, the results of Gal et al. (12) are not directly applicable to hydrosol filtration. However, just as explicitly including the effects of grain interaction has advanced the understanding and accuracy of aerosol modeling, similar rewards may lie in the application of the concept to hydrosols.

In the clean bed models discussed above, model-predicted effects of particle size and surface chemistry deviate significantly from experimental results. In general, experimentally measured collection of small particles is greater than predicted, and collection of large particles is less than predicted (14, 15). Another area of disagreement between observed behavior and predictions of current models is the effect of surface chemistry on particle removal. Current models predict a step decrease in removal as surface chemistry becomes unfavorable, whereas observations show a gradual decrease.

Due to the presence of contact points, an array of spheres shares critical geometric features with a packed bed. Consider the effect of grains in contact on the critical trajectory (or trajectory defining regions of fluid flow in which particles are or are not predicted to collide with the collector) as

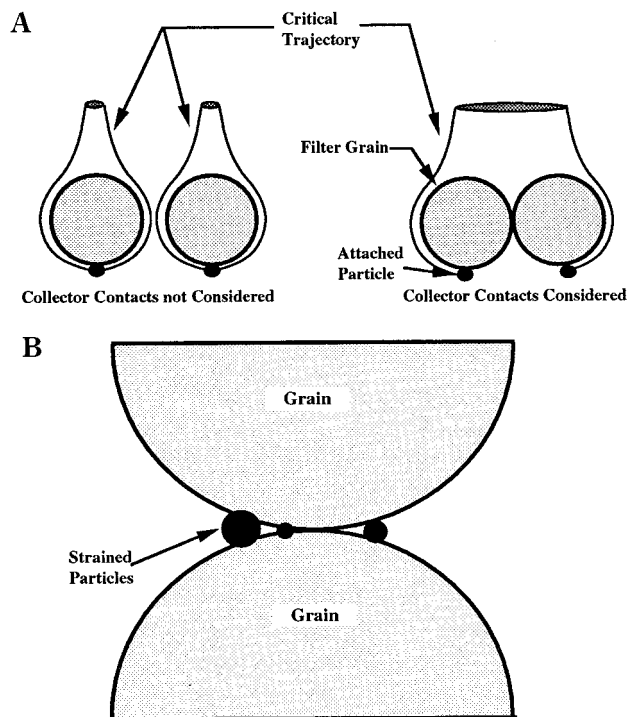


FIGURE 1. Geometric ramifications of filter grain contact points. (A) Influence of collector contact points on critical area. (B) Conceptual view of collector contact straining.

illustrated in Figure 1A, after Gal et al. (12); two collectors in contact produce more collisions than the sum of collisions for two separated collectors. Currently, three conceptual mechanisms for particle collection are reported in the literature: sedimentation, gravity force causing a particle to cross streamlines; interception, a particle traveling on a streamline passing within one particle radius of the surface of a collector; and Brownian motion, random Brownian motion or diffusion causing a particle to cross streamlines and collide with a collector. Figure 1B illustrates a collection mechanism (collector contact straining) that is possible in an actual packed bed and in the AOS media model but not in previously applied models. In general, straining as a particle separation mechanism is not sensitive to surface chemistry. Although collector contact straining is limited to a small fraction of the bed, high removal efficiency over a small fraction of the available bed may be significant overall, particularly when surface chemistry is unfavorable. Although not addressed in this paper, collection in the region near grain contact points also has ramifications with regard to deposit distribution, morphology, head loss development, and other dynamic aspects of filtration.

**Model Development.** The actual random packing within a filter is extremely cumbersome to deal with mathematically; however, regular (periodic) packing schemes allow symmetry to be developed that simplifies and compresses the mathematical representation. Several researchers have presented mathematical solution methods for flow through regular geometric packing arrangements (including refs 13, and 17–20). The porous media model of Snyder and Stewart (13) was used in this work, and the dense cubic packing arrangement and associated coordinate system are illustrated in Figure 2, after Snyder and Stewart (13). Details regarding the development of the porous media model are available elsewhere (13, 21, 22).

With media model and associated flow field established, the deterministic component of the trajectory of a particle can be determined by resolving the forces and torques acting on the particle. A schematic representation of the forces

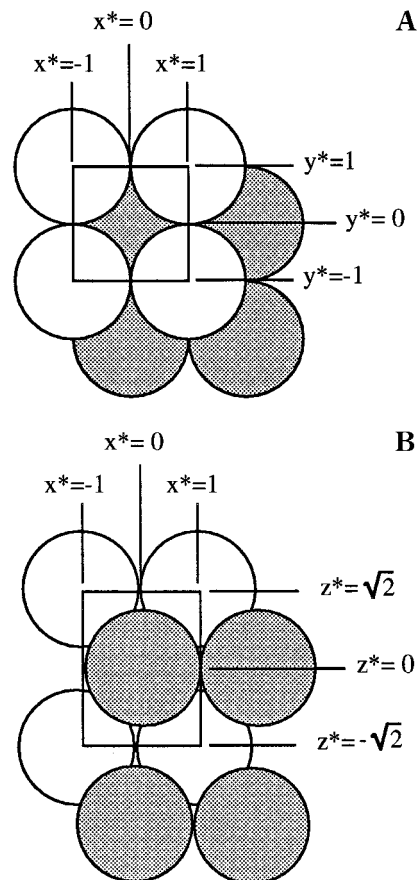


FIGURE 2. Array-of-spheres media model and associated coordinate system (after ref 13). (A) Top view. (B) Side view.

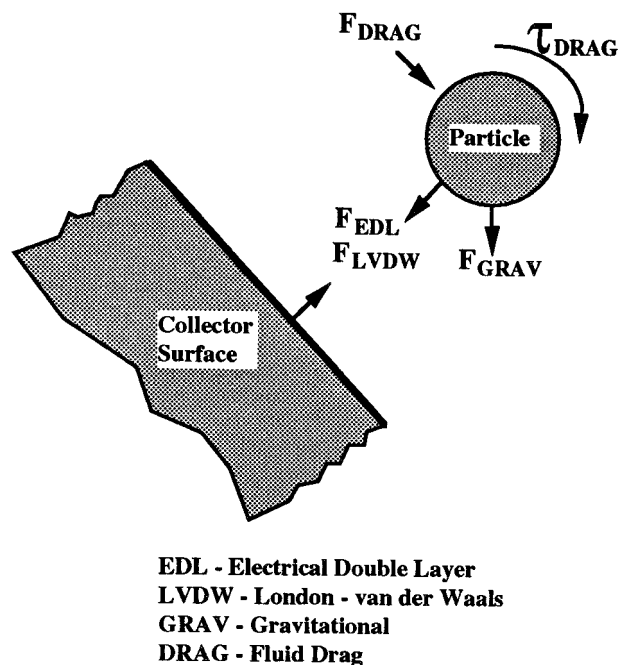


FIGURE 3. Forces and torques considered in the trajectory analysis.

and torques considered in this research is presented in Figure 3. In the model discussed herein and other trajectory models of aqueous depth filtration, particle inertia is assumed negligible, particles and media grains are assumed spherical (given the size differential between particles and media grains, sphere-plane systems are assumed for some close range interactions), and all forces act through the center of the

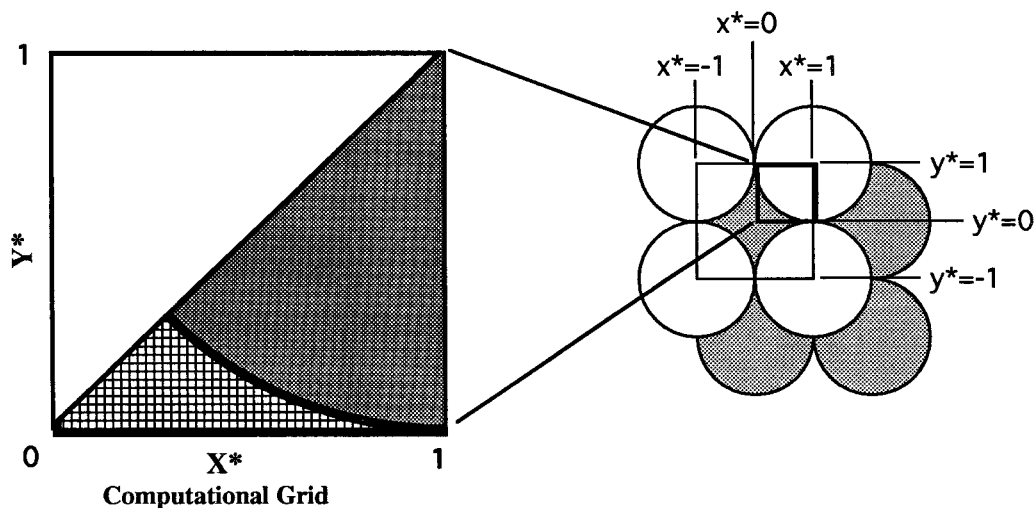


FIGURE 4. Conceptual view of the trajectory computational grid.

particles except close range hydrodynamic interactions. Forces considered in this work are gravity and buoyant forces, drag (through Stokes' law—corrected at close range to collector surfaces), electrical double-layer repulsion, and London–van der Waals interaction. As a particle approaches a surface, additional fluid drag is encountered. The shear force acting on the particle surface facing the collector is different than that acting on the particle surface facing the free fluid. This difference in shear forces creates a torque and hence rotation, and at close range to a collector surface, a torque balance is also applied.

The critical area is the planar region perpendicular to bulk flow within which all trajectories result in predicted collision with the collector. The ratio of the integral of particle flux through the critical area to the integral of particle flux through the entire region being considered is predicted particle removal efficiency. In previously applied models, the critical area is circular because of the symmetry of spherical and tubular collectors. Hence, computation of one trajectory (the critical trajectory) is sufficient to determine the critical area in these media models. The critical trajectory is traditionally determined through backward integration from the rear stagnation point in spherical media models or the trailing tube boundary in constricted tube models. The critical area and particle flux in the AOS model is irregular, and numerous trajectories must be determined to define the boundaries of the area.

To compute unit cell efficiency, one-eighth of the top plane of the unit cell was divided into a computational grid. A computer algorithm was developed that determined the boundary of the critical area by evaluating trajectory results. Particle trajectories were calculated from a starting value of  $z = \sqrt{2}$  to  $z = -\sqrt{2}$  or until the particle collided with a media grain or became effectively immobilized in a secondary minimum. The integral of the product of area and velocity normal to the computational grid is equivalent to particle flux into the unit cell for a homogeneous suspension. The unit cell efficiency was thus determined as the ratio of flux through the critical area to total flux through the computational grid. A conceptual illustration of the computational grid is shown in Figure 4. A sensitivity analysis was performed on grid resolution, and considering sensitivity and computational expense, a grid resolution of 240 divisions per collector radius was selected.

The particle trajectory is defined by two first-order ordinary differential equations. These equations were solved using a fifth-order Runge–Kutta method with variable step size (23) coded in FORTRAN. Program development was

performed on a 486-PC; reported results were calculated at single precision on a Cray Y/MP computer. Impact of numerical method tolerance was examined; solutions coincide for tolerances less than or equal to  $10^{-8}$ .

## Results and Discussion

**Qualitative Trends.** Critical collection regions under various conditions are shown in Figure 5. As discussed above, trajectories were calculated for particles originating at the position  $z = \sqrt{2}$  and at each  $X^*$  and  $Y^*$  location as indicated in the computational grid of Figure 4. The fate, i.e., passage or collection, of particles defines the critical collection region. All particles originating inside the region are collected, while those outside pass through the cell. Thus, the collection efficiency is related to the area associated with the critical collection region. For example, a collection efficiency of zero would have no critical collection region, and a plot of the form shown in Figure 5 would have no shading; conversely, if a collection efficiency were 100%, the entire plot would be shaded. Because of the symmetry of the AOS unit cell, the critical collection region for only one-quarter of the unit cell is shown.

The critical areas of the AOS model, as shown in Figure 5, are more complex than the circular critical areas of previously applied media models but do possess a degree of symmetry. Areas of collection consist of a central collection region with areas extending away from the center as “spokes” from the origin in the  $x$  and  $y$  directions and at a slope of 1. The directions of these spokes correspond to locations of collector–collector contact points within the AOS cell and represent collection associated with filter grain contact points.

Figure 5A illustrates the effect of change in velocity on critical area (and hence removal efficiency). Critical areas are shown for collection of a  $6.3 \mu\text{m}$  diameter particle by a 1.85 mm diameter filter grain at approach velocities of 0.5 mm/s (0.7 gpm/ft<sup>2</sup>) and 5.5 mm/s (7.9 gpm/ft<sup>2</sup>). Other parameter values used in the simulations include temperature of 25 °C and a Hamaker's constant of  $1.0 \times 10^{-15} \text{ g}\cdot\text{cm}^2/\text{s}^2$ . Critical area decreases as velocity increases, meaning that removal decreases with increasing velocity, as expected. As the area of the critical region decreases, the characteristic shape is maintained.

The effect of particle diameter on critical area is shown in Figure 5B. For media grain size of 1.85 mm, approach velocity of 0.45 mm/s (0.7 gpm/ft<sup>2</sup>), and other parameters constant, critical areas for 1.0  $\mu\text{m}$  and 6.3  $\mu\text{m}$  diameter particles are shown. The figure shows that critical area decreases as particle size decreases, indicating the expected

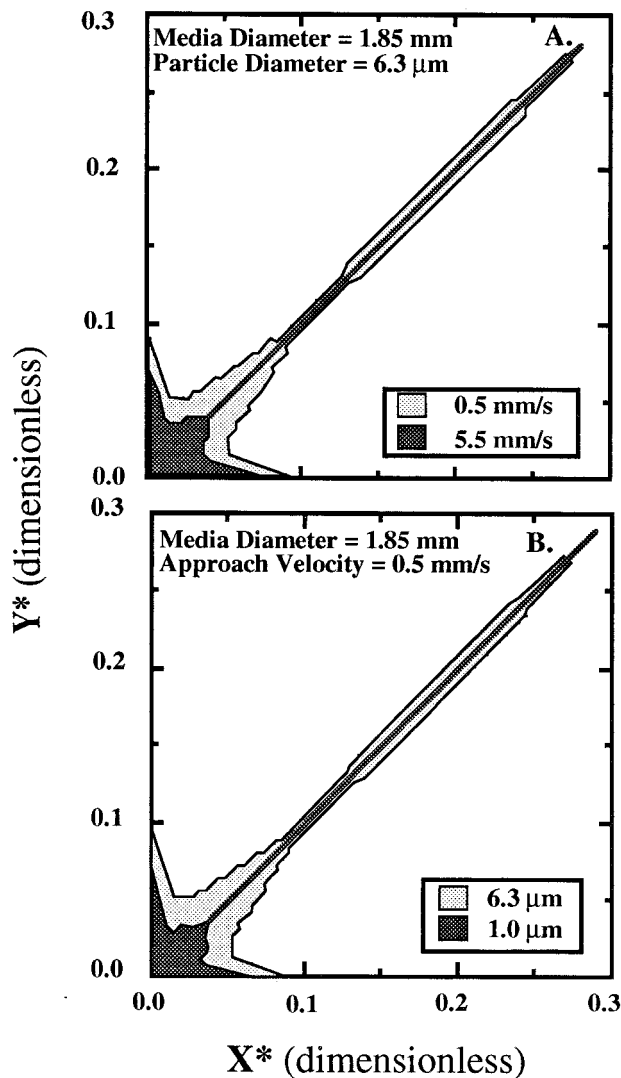


FIGURE 5. Characteristic shape of critical collection region.

inverse relationship between particle size and removal for non-Brownian particles. Again, the characteristic shape of the critical area, with collection coincidental with contact points and central region, is maintained.

Predicted single collector efficiency for a range of particle diameters ( $d_p$ ) and two media diameters (0.8 and 1.8 mm) at an approach velocity of 1.8 mm/s (2.8 gpm/ft<sup>2</sup>) is shown in Figure 6. The general trend for both media sizes is increasing single collector efficiency with increasing particle diameter, although a slight minimum exists at approximately  $\log(d_p) = 0.2$  ( $d_p = 3 \mu\text{m}$ ). Trajectory calculations were strictly deterministic; Brownian, or diffusional, influence was not included. Hence, this particle size of minimum removal is not caused by the classic effect of diminishing Brownian transport with increasing particle size. Using other porous media models, similar minimums have been identified previously (14). This minimum is caused by counteracting effects of enhanced collision opportunity by (primarily) interception and increased hydrodynamic retardation as particle size increases. For the larger media size ( $d_c = 1.8$  mm), the location of this minimum in single collector efficiency occurs at a slightly greater particle size. The larger media size also exhibits significantly greater single collector efficiency at larger particle sizes ( $\log d_p > \sim 1$ ;  $d_p > \sim 10 \mu\text{m}$ ). Both of these phenomena are caused by the lower hydrodynamic interaction associated with the larger interstitial space of the larger media.

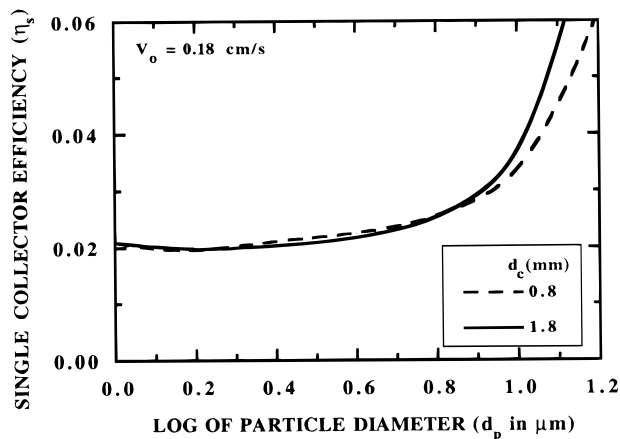


FIGURE 6. Model sensitivity to media size.

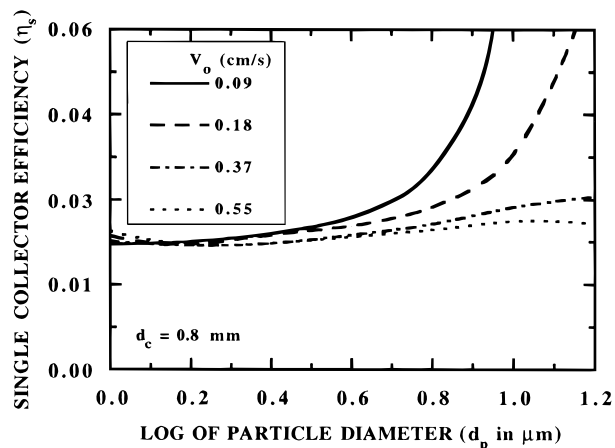


FIGURE 7. Model sensitivity to approach velocity.

Sensitivity of the model to changes in approach velocity is illustrated in Figure 7. Removal decreases with increasing velocity, as expected. As velocity increases, the dependence on particle diameter is reduced. This reduced dependence is caused by two coupled effects. First, hydrodynamic interaction increases as approach velocity increases. Second, larger particles are effected to a greater extent by these hydrodynamic influences. As with the media size comparison above, a slight minimum exists at about  $3 \mu\text{m}$  ( $\log d_p = 0.2$ ). At the highest velocity (5.5 mm/s), a slight maximum is evident at about  $10 \mu\text{m}$  ( $\log d_p = 1.0$ ); this is again caused by counteracting interception collection and hydrodynamic retardation. In trajectory modeling, a maximum in the relationship between clean bed removal and particle diameter has not been reported previously. Mackie et al. (23), however, noted a similar trend during dynamic simulation after significant deposition has taken place. Because of the lower porosity, the interstitial velocity and hence hydrodynamic interaction is greater in the AOS model than in spherical or tubular models as they have been applied to trajectory analysis. The relationship between removal in the low porosity, densely packed unit cell of the AOS media model and the greater porosity, randomly packed bed of a filter is discussed subsequently.

A comparison of AOS model, Happel's model, and experimental response to changes in electrical double-layer repulsion is presented in Figure 8. The ordinate of the plot is the logarithm of the ratio of single collector efficiency under a given chemical condition ( $\eta$ ) to single collector efficiency under ideal chemical conditions ( $\eta_o$ ). An ordinate value of zero (i.e.,  $\eta/\eta_o = 1$ ) represents removal under ideal conditions, and relative removal decreases as ordinate values decrease.

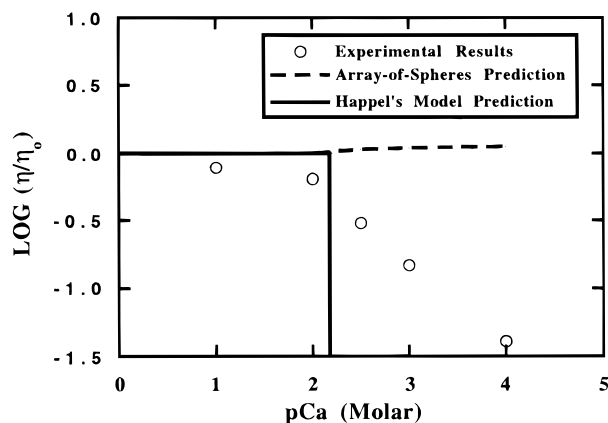


FIGURE 8. Effect of surface chemistry on trajectory model predictions (Happel's model prediction and experimental results from ref  $\delta$ ).

The abscissa is the negative logarithm of the calcium ion concentration. As abscissa values increase, calcium concentration decreases and electrical double-layer repulsion increases. Trajectory analysis applied to Happel's sphere-in-cell model (solid line) predicts an abrupt (almost step) decrease in removal at some critical value of calcium concentration ( $\theta$ ); this sharp decrease in predicted removal coincides with the onset of a net repulsive force between particle and media. The experimental results ( $\theta$ ) show a much more gradual decline as chemical conditions deteriorate. These trends are consistently reported for other currently used porous media models (constricted tube and isolated sphere) and other experimental results. Removal predictions based on the AOS porous media model (dashed line), however, remain basically unchanged as electrical double-layer repulsion increases. This total lack of sensitivity is an artifact of the AOS model. A particle close enough to a sphere to experience specific hydrodynamic influence drifts in the direction of least velocity. In the AOS media model, velocity in the bulk fluid has a minimum corresponding to locations of grain contact points. Even when a net repulsion exists that does not allow attachment of particles to collectors, the particles are "funneled" toward collector contact points and become hydrodynamically trapped. In an actual packed bed, a number of variables would preclude or severely limit this type of collection: random packing within an actual bed as opposed to the cubic symmetry of the AOS media model, nonspherical collectors and particles, Brownian motion of particles, and deviation of the fluid flow regime from the creeping flow assumption.

Although collection in secondary minima is damped by these nonidealities, migration toward contact points likely occurs to some extent in actual packed beds during both favorable and unfavorable surface chemistry conditions. Photographic evidence (25) shows a majority of retained particles located near grain contact points. Similar observations were made through the Plexiglas walls of laboratory-scale filter columns during experiments performed in the authors' laboratory; note, however, that wall effects may prevent any conclusive statement using this type of observation technique. These observations are indicative of migration toward grain contact points. However, whether the migration occurs in the bulk fluid during transport to the collector or along the surface after collision cannot be inferred. Only the former case is considered in the current modeling effort; however, Clark et al. (26) speculated that migration along grain surfaces after collision might occur.

**Comparison to Experimental Data.** To calculate removal in a filter, output of the trajectory model (single collector efficiency,  $\eta_s$ ) must first be converted to filter coefficient ( $\lambda$ ). The transformation from single collector efficiency to filter

coefficient entails compensating for the difference between the porosity of the media model and that of the actual filter bed. The low porosity in the densely packed media model can be compensated for by supplying additional void volume in parallel. This method shares the idea of parallel flow distribution within the bed with Payatakes and Tien's (27) unit bed element concept of the filter bed. In their approach, parallel elements can have different sizes and/or geometries, but each individual element has the same porosity as the entire bed. In an actual randomly packed filter bed, the packing density varies spatially, between densely packed regions and bridged, relatively void regions.

Constraints and assumptions of the derivation of the relationship between single collector efficiency and filter coefficient with parallel flow distribution are as follows:

(a) The deficit in porosity is accounted for by additional void space acting in parallel with the AOS unit cell.

(b) The additional void space is represented as a capillary tube of length equal to that of the AOS unit cell.

(c) Diameter of the void tube is such that resulting overall porosity is equal to that of the packed bed.

(d) Flow distribution is such that head loss across the void tube and the AOS unit cell is equal.

(e) No particle collection occurs in the void tube. Applying the above constraints and assumptions, the ratio of fluid flowing into the AOS unit cell ( $Q_{AOS}$ ) to fluid flowing into the entire bed ( $Q_{total}$ ) is found to be

$$\frac{Q_{AOS}}{Q_{total}} = \theta = \frac{\epsilon_{AOS}^3}{22.5\pi(1 - \epsilon_{AOS})^2 \left[ \frac{1}{3\sqrt{2}(1 - \epsilon_{total})} - \frac{1}{\pi} \right]^2 + \epsilon_{AOS}^3} \quad (8)$$

where  $\epsilon_{AOS}$  is the porosity of the AOS model—0.26 for the dense cubic packing of spheres and  $\epsilon_{total}$  is the porosity of the randomly packed bed—0.39 for the following comparisons. A detailed derivation of the above relationship is available elsewhere (22). Given the assumption that the influent particle concentration to any section of the filter is homogeneous, the flow distribution ratio ( $\theta$ ) represents the fraction of particles entering a filter section that pass into the AOS unit cell.

In the parallel void deficit compensation scheme, single collector efficiency ( $\eta_s$ ) is related to filter coefficient by

$$\lambda_{AOS} = \frac{\theta \eta_s}{\sqrt{2} d_c} \quad (9)$$

Since only a fraction of the total flow into the filter passes through the AOS unit cell, the superficial velocity of the AOS unit cell is different than that of the entire filter. The relationship between superficial velocity of the filter ( $V_o$ ) and the superficial velocity of the AOS unit cell ( $u_{AOS}$ ) was derived under the assumptions and constraints listed above (22). The resulting relationship is

$$u_{AOS} = \theta V_o \left( \frac{\pi}{3\sqrt{2}(1 - \epsilon)} \right) \quad (10)$$

The AOS unit cell superficial velocity is the velocity that influences particle trajectories within the AOS porous media model. For any given filtration rate, the corresponding AOS unit cell superficial velocity must be used to calculate particle trajectories and removal.

To facilitate use of the trajectory results, a correlation for single collector efficiency was developed. As shown above, modeling of the effect of surface chemistry was not successful; hence, the correlation is based on trajectory results with no electrical double-layer interaction. The relationship among

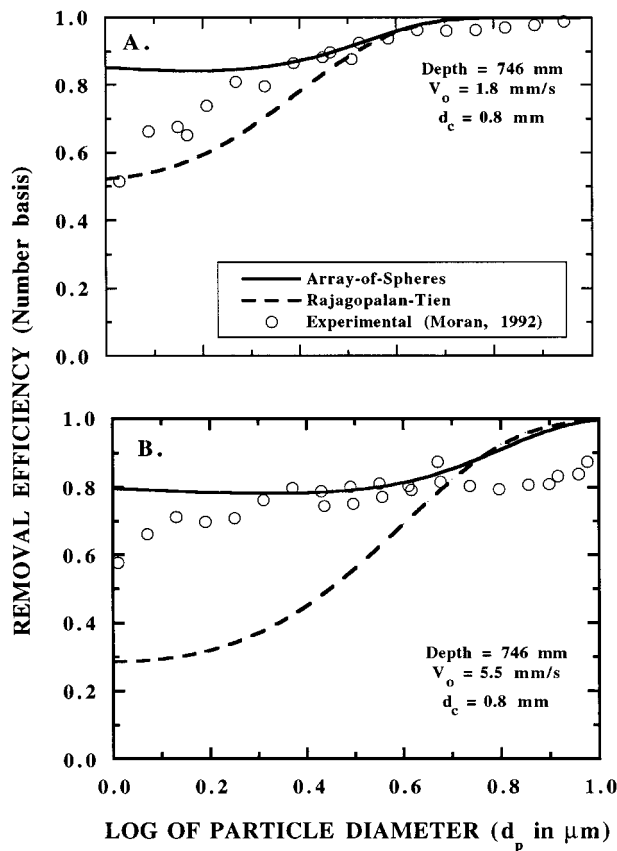


FIGURE 9. Effect of velocity: comparison among Rajagopalan-Tien and AOS models and results of ref 16.

the dimensionless groups  $N_{Lo}$ ,  $N_G$ , and  $N_R$  proposed by Rajagopalan and Tien (4) was used (presented above as eqs 2-6).

Nonlinear multivariate regression analysis was performed using the statistical package *SPSS for Windows* (27, 28) on a PC/486 microcomputer. The regression was performed using the Levenberg-Marquardt Method (24). Data used for the regression represented particle diameters between 1 and 15  $\mu\text{m}$ , particle densities of 1.05 and 2.45  $\text{g}/\text{cm}^3$ , media diameters from 0.4 to 1.8 mm, and approach velocities from 0.9 to 7.5 mm/s (1.3 to 10.8  $\text{gpm}/\text{ft}^2$ ).

Inserting the resulting coefficient and exponent values, the non-Brownian single collector efficiency of the AOS is

$$\eta_s = 0.029N_{Lo}^{0.012}N_R^{0.023} + 0.48N_G^{1.8}N_R^{-0.38} \quad (11)$$

The correlation represents the direct model results well, with an  $r^2$  value of 0.98.

Brownian motion is also important to the transport and collection of particles on the order of 1  $\mu\text{m}$  and smaller. However, introduction of Brownian transport (diffusion) leads to nondeterministic behavior and results in trajectories defined by stochastic differential equations. The problem is traditionally decoupled using the assumption that the Brownian and deterministic transport mechanisms are additive. The arguments presented above showing the need for a more realistic media model are less important for diffusion dominated particles. Since Brownian motion causes random particle displacement, trajectories of such particles are not so highly coincidental with fluid streamlines. Thus a model that accounts for neighboring collectors in a spatially averaged manner, such as Happel's model, is appropriate for Brownian collection dominated particles. Cookson's solution for convective diffusion in Happel's sphere-in-cell model (10; presented above as eq 7) was used

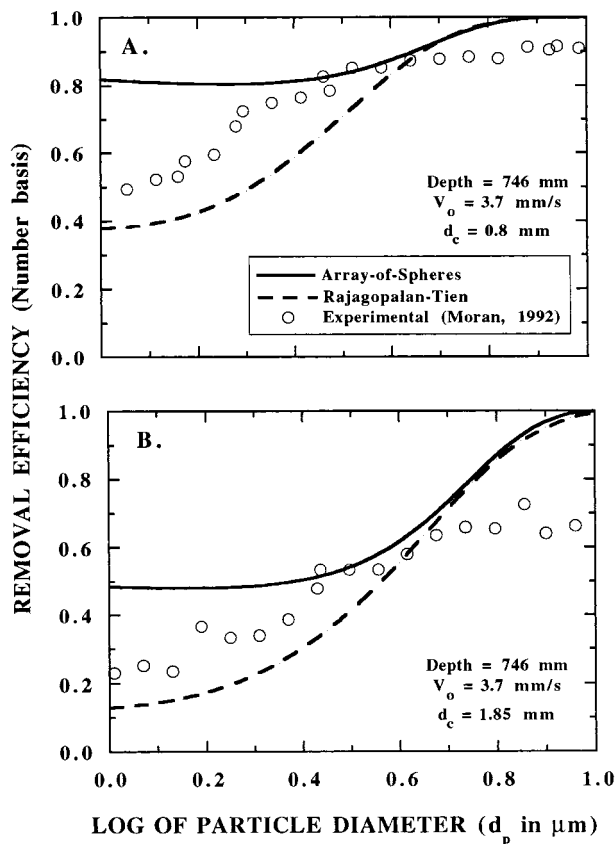


FIGURE 10. Effect of media size: comparison among Rajagopalan-Tien and AOS models and results of ref 16.

by Rajagopalan and Tien (4) and is also used for the following experimental and model comparisons.

Below, comparisons are made among AOS and Rajagopalan-Tien models and the experimental results of Moran et al. (16). Experimental data were collected during laboratory-scale filtration experiments using effluent samples from the sedimentation basins of a lime-softening water treatment plant. Elevated pH ( $\sim 10$ ) and the addition of ferric chloride during rapid mix ensured favorable particle surface chemistry; hence, electrical double-layer interactions are assumed negligible. The particles consisted primarily of calcium carbonate, and for the model input, particle density of 2.45  $\text{g}/\text{cm}^3$  was assumed, and temperature of 25  $^\circ\text{C}$  and Hamaker's constant of  $1.0 \times 10^{-13} \text{ g}\cdot\text{cm}^2/\text{s}^2$  were used.

Figure 9 illustrates a comparison of the AOS and Rajagopalan-Tien models and experimental results at two different velocities (1.8 and 5.5 mm/s for parts A and B, respectively) and with a media size of 0.8 mm. Figure 9A shows results at a relatively low approach velocity (1.8 mm/s). The Rajagopalan-Tien model underpredicts small particle removal and overpredicts large particle removal—results typical of sphere-in-cell-based trajectory models. The AOS model tends to overpredict removal for all particle sizes, although good agreement is evident in the intermediate size range of 2-4  $\mu\text{m}$  ( $0.3 < \log d_p < 0.65$ ). Sensitivity to particle size is weaker for the AOS model, with removal efficiency high for the smallest particles shown and gradually increasing to (effectively) unity by  $\log d_p$  of 1 (10  $\mu\text{m}$ ). Because the Rajagopalan-Tien model exhibits greater sensitivity to particle size, the two models converge and, under these conditions, coincide for particles greater than about 3.76  $\mu\text{m}$  ( $\log d_p = 0.575$ ).

Figure 9B shows a comparison at a relatively high approach velocity (5.5 mm/s). The removal trends are similar to part A. However, the Rajagopalan-Tien model does not

represent this higher velocity as well, while the AOS Model appears to represent this condition better than the lower velocity (1.8 mm/s; Figure 9A). Both models still overpredict large particle removal, and the AOS correlation still overpredicts the low end of the range shown ( $\log d_p < 0.15$ ). At the higher velocity, the models again converge; however, the particle size at which they meet is greater,  $d_p = 5.6 \mu\text{m}$  ( $\log d_p = 0.75$ ).

The Rajagopalan–Tien model shows a much greater change in predicted removal with change in velocity than either the AOS model or the experimental results. The AOS model's lack of sensitivity to changes in approach velocity for small particles is evident in comparing Figure 9, panels A and B. The experimental results show a similar lack of sensitivity to this change in velocity.

Figure 10 shows a comparison of the models and experimental results for two media sizes. The trends identified in Figure 9 are also evident in Figure 10. Media size has a more significant impact on both models and experimental results than velocity. Comparison of parts A and B of Figure 10 shows that relative sensitivity to these media sizes is similar for both models and the experimental results for smaller particle sizes. However, the models are less sensitive to media size change for larger particles than are the experimental results. The models tend to bracket the experimental results of smaller particles, but both overpredict removal of larger particles. Overprediction of removal of larger particles by both models is greater for the larger media size (1.85 mm; part B). This overprediction leads to poorer representation of large particle removal by both models at the larger media size.

## Discussion

Deep bed filtration represents a major challenge with respect to mathematical modeling. In reality, filters have random packing with highly complex flow fields, even in highly idealized laboratory-scale reactors with uniform spheres as the packing media. At this time, mathematical modeling cannot capture completely the breadth of complexity present in real filters. The model developed in this paper represents a first attempt to capture some of the complexity associated with the fact that filter grains are in contact with one another. These grain contact points influence flow field and collector geometry and therefore should influence the removal of particles. Previous filtration models based on a single collector (sphere or tube) approach have included the net or average effect of neighboring collectors on flow (and head loss) through, for example, the use of Happel's model, but all to date have ignored the direct effect of contact points.

To consider contact points, the model developed in this research necessarily had its own set of idealized conditions. One primary idealization was the choice of the dense cubic packing arrangement of spherical filter grains, a choice made, among other reasons, because the flow field had been solved by previous investigators. The flow field solution of Snyder and Stewart (13) is itself an approximation, a correlation approximating the conditions set forth by the geometry, Navier–Stokes equation under creeping flow, and the continuity equation. The dense packing required, in turn, a porosity correction, and like the Happel model, it is correct for the net or average flow and head loss but imposes error in terms of particle capture. While aware of that potential error and the idealizations, the authors believe the assumptions and methodology provide some insight, at least qualitatively, to particle capture in filtration that cannot be obtained from models that ignore contact points.

The model suggests, first, that contact points do influence capture of particles and to a significant degree. This result is not a simple factor of straining (particles too large to fit through the small spaces near contact points) but of complex

hydrodynamics that funnel particles toward contact points and also make the region near contact points stable regions of collection—forces on particles are balanced in these regions, immobilizing them. Second, the model results give ranges of particle size (and possibly filtration velocity and particle density) in which capture is much less effected by these variables than previous models. Experimental results, not only from our own laboratory (16) but from others like the classic results of FitzPatrick and Spielman (30), suggest that previous models such as Rajagopalan and Tien (4, 5) might be overly sensitive to these variables—i.e., the models show greater sensitivity to these variables than is found experimentally. The model proposed in this paper is apparently less sensitive to these variables than is found experimentally; reality seems to lie somewhere between the predictions of the two types of models.

The model also is, quite clearly, imperfect—the fact that the results (at least in the ranges chosen for this study) are insensitive to chemical effects is a serious deficiency. This result might be an artifact of the idealized geometry model that leads to particle stagnation points based on hydrodynamics alone. Real filters with random packing do not have these points of symmetry that cause the mathematical result. Again, existing models overpredict the sensitivity to chemical conditions whereas this model underpredicts that sensitivity.

In summary, the model developed in this paper shows promise while still requiring further development. Filtration modeling that explicitly accounts for the detailed flow field around collectors, including the effects of contact points among adjacent collectors, apparently correctly accounts (at least qualitatively) for and provides some insight into some phenomena that are observed in real filters.

## Acknowledgments

This research was supported by the U.S. Environmental Protection Agency (U.S. EPA) Office of Research and Development, under Grant R-816746-01 to D.F.L. The ideas and conclusions of the paper are those of the authors alone and do not necessarily reflect opinions of the U.S. EPA. We are grateful to students whose experimental work and thoughtful contributions on filtration aided and guided this research. Of particular note are Jeannie Darby, Sarah Clark, Melissa Moran, and Dan Moran. The authors also appreciate the suggestions of the reviewers, whose ideas and perspectives improved the final manuscript considerably.

## Supporting Information Available

Hydrodynamics aspects of the porous media model used for the AOS filtration model (26 pages). Ordering information is given on current masthead page.

## Literature Cited

- (1) Iwasaki, T. *J. Am. Water Works Assoc.* **1937**, *29* (10), 1591–1602.
- (2) Yao, K.; Habibian, M. T.; O'Melia, C. R. *Environ. Sci. Eng.* **1971**, *5* (11), 1105–1112.
- (3) Spielman, L. A.; FitzPatrick, J. A. *J. Colloid Interface Sci.* **1973**, *42*, (3), 607–623.
- (4) Rajagopalan, R.; Tien, C. *AIChE J.* **1976**, *22* (3), 523–533.
- (5) Rajagopalan, R.; Tien, C.; Pfeffer, R.; Tardos, G. *AIChE J.* **1982**, *28* (5), 871–872.
- (6) Tobiason, J. E.; O'Melia, C. R. *J. Am. Water Works Assoc.* **1988**, *80* (12), 54–64.
- (7) Happel, J. *AIChE J.* **1958**, *4* (2), 197–201.
- (8) Payatakes, A. C.; Tien, C.; Turian, R. M. *AIChE J.* **1974**, *20* (5), 889–900.
- (9) Payatakes, A. C.; Tien, C.; Turian, R. M. *AIChE J.* **1974**, *20* (5), 900–905.
- (10) Cookson, J. T. *Environ. Sci. Technol.* **1970**, *4* (2), 128–134.
- (11) Vitthal, S. A Model for Particle Deposition and Filter Cake Buildup in Granular Media. Ph.D. Dissertation, University of Texas at Austin, 1991.
- (12) Gal, E.; Tardos, G.; Pfeffer, R. *AIChE J.* **1985**, *31* (7), 1093–1104.

- (13) Snyder, L. J.; Stewart, W. E. *AIChE J.* **1966**, *12* (1), 167–173.
- (14) Tien, C. *Granular Filtration of Aerosols and Hydrosols*, Vol. 1; Butterworth Series in Chemical Engineering; Howard, B., Ed.; Butterworth Publishers: Stoneham, MA, 1989.
- (15) James M. Montgomery, Consulting Engineers, Inc. *Water Treatment Principles and Design*; Wiley-Interscience: New York, 1985.
- (16) Moran, D. C.; Moran, M. S.; Cushing, R. S.; Lawler, D. F. *J. Am. Water Works Assoc.* **1993**, December.
- (17) Hasimoto, H. *J. Fluid Mechan.* **1959**, 317–328.
- (18) Sørensen, J. P.; Stewart, W. E. *Chem. Eng. Sci.* **1974**, *29*, 819–825.
- (19) Zick, A. A.; Homsy, G. *J. Fluid Mechan.* **1982**, *115*, (1) 13–26.
- (20) Sangani, A. S.; Acrivos, A. *Int. J. Multiphase Flow* **1982**, *8* (4), 343–360.
- (21) Gal, E. Dust Filtration in Granular Beds. Ph.D. Dissertation, The City University of New York, 1984.
- (22) Cushing, R. S. Mathematical Modeling of Depth Filtration: Investigation of Initial Removal Through Three-Dimensional Trajectory Analysis. Ph.D. Dissertation, The University of Texas at Austin, 1993.
- (23) Mackie, R. I.; Horner, R. M. W.; Jarvis, R. J. *AIChE J.* **1987**, *33* (11), 1761–1775.
- (24) Press, W. H.; Flannery, B. P.; Teukolsky, S. A. Vetterling, W. T. *Numerical Recipes: The Art of Scientific Computing*, Cambridge University Press: Cambridge, MA, 1989.
- (25) Cleasby, J. L. Chapter 8: Filtration In *Water Quality and Treatment*; McGraw-Hill: New York, 1990.
- (26) Clark, S. C.; Lawler, D. F.; Cushing, R. S. *J. Am. Water Works Assoc.* **1992**, *84* (12), 61–71.
- (27) Payatakes, A. C.; Tien, C.; Turian, R. M. *AIChE J.* **1973**, *19* (1), 58–67.
- (28) Norusis, M. J. *SPSS for Windows: Base System User's Guide—Release 6.0*; SPSS Inc.: Chicago, IL, 1993.
- (29) Norusis, M. J. *SPSS for Windows: Advanced Statistics—Release 6.0*; SPSS Inc.: Chicago, IL, 1993.
- (30) FitzPatrick, J. A.; Spielman, L. A. *J. Colloid Interface Sci.* **1973**, *43*, 350–369.

*Received for review August 26, 1997. Revised manuscript received July 1, 1998. Accepted August 21, 1998.*

ES9707567